Neurobiology of Disease 82 (2015) 213–225

Contents lists available at ScienceDirect

Neurobiology of Disease

journal homepage: www.elsevier.com/locate/ynbdi

Hypoglycemia-induced alterations in hippocampal intrinsic rhythms: Decreased inhibition, increased excitation, seizures and spreading depression

C.M. Florez [a,b], V. Lukankin [a], S. Sugumar [a], R. McGinn [a], Z.J. Zhang [a], L. Zhang [a], P.L. Carlen [a,b,*]

[a] Departments of Medicine (Neurology) and Physiology, University of Toronto, Toronto, Canada
[b] Division of Fundamental Neurobiology, TWRI, UHN, Toronto, Canada

ARTICLE INFO

Article history:
Received 9 November 2014
Revised 9 June 2015
Accepted 12 June 2015
Available online 18 June 2015

Keywords:
Hippocampus
In-vitro
Seizure
Spreading depression
Hypoglycemia
Neuroglycopenia
In-vitro brain rhythms
Brain oscillations

ABSTRACT

Seizures are the most common clinical presentation of severe hypoglycemia, usually as a side effect of insulin treatment for juvenile onset type 1 diabetes mellitus and advanced type 2 diabetes. We used the mouse thick hippocampal slice preparation to study the pathophysiology of hypoglycemia-induced seizures and the effects of severe glucose depletion on the isolated hippocampal rhythms from the CA3 circuitry.

Methods and results: Dropping the glucose perfusate concentration from the standard 10 mM to 1 mM produced epileptiform activity in 14/16 of the slices. Seizure-like events (SLEs) originated in the CA3 region and then spread into the CA1 region. Following the SLE, a spreading-depression (SD)-like event occurred (12/16 slices) with irreversible synaptic failure in the CA1 region (8/12 slices). CA3 SD-like events followed ~30 s after the SD-like event in the CA1 region. Less commonly, SD-like events originated in the CA3 region (4/12). Additionally, prior to the onset of the SLE in the CA3 area, there was decreased GABA correlated baseline SPW activity (bSPW), while there was increased large-amplitude sharp wave (LASW) activity, thought to originate from synchronous pyramidal cell firing. CA3 pyramidal cells displayed progressive tonic depolarization prior to the seizure which was resistant to synaptic transmission blockade. The initiation of hypoglycemic seizures and SD was prevented by AMPA/kainate or NMDA receptor blockade.

Conclusions: Severe glucose depletion induces rapid changes initiated in the intrinsic CA3 rhythms of the hippocampus including depressed inhibition and enhanced excitation, which may underlie the mechanisms of seizure generation and delayed spreading depression.

Introduction

Hypoglycemia is a leading cause of neurological sequelae in infants suffering from severe metabolic or infectious disorders (Montassir et al., 2009), and the most common side effect of insulin treatment in individuals with type 1 diabetes (Cryer, 2010) and insulin-dependent type 2 diabetes (Avila-Fematt and Montana-Alvarez, 2010). Seizures are the most common clinical presentation (>80%) of severe neonatal hypoglycemia, with glucose levels usually below 2 mM (Burns et al., 2008). EEG recordings in humans and in animal models of hypoglycemia show a pattern of decreased alpha and beta activity, large delta waves (Auer et al., 1984), spike and bursting activity (Gibbs and Murray, 1954), seizures, and finally isoelectricity (Lewis et al., 1974).

The anterior temporal lobe and hippocampus are among the most epileptogenic areas of the brain and have been implicated as possible trigger zones for hypoglycemic seizures (Baloyannis et al., 1987; Gibbs and Murray, 1954; Lapenta et al., 2010), although in vivo EEG recordings have not clearly established the areas of seizure origin (Del Campo et al., 2009; Gibbs and Murray, 1954; Velisek et al., 2008). It is clear that severe hypoglycemia can lead to neuronal death predominantly in the hippocampus and in the superficial layers (layers II–III) of the occipital and parietal cortices, and striatum (Auer, 2004; Auer et al., 1985a; Auer et al., 1985b; Bree et al., 2009). This pattern of damage seems to be related to the direct effects of massive release of aspartate and glutamate (Auer, 2004). After severe hypoglycemia, there is cellular degeneration in the dentate gyrus (DG) and CA1, with less involvement of the CA3 region (Auer, 2004; Shin et al., 2010). The reasons for this difference in regional cellular survival in the hippocampus are not well understood. Functionally, in vitro hypoglycemic experiments showed that the CA1 region is susceptible to synaptic failure (Abdelmalik et al., 2007; Crepel et al., 1992; Fan et al., 1988; Sadgrove et al., 2007), an effect exacerbated by the presence of seizures (Abdelmalik et al., 2007).

Abbreviations: bSPW, baseline sharp wave; LASW, large amplitude sharp wave; SLE, seizure-like event; SD, spreading depression-like event.

* Corresponding author at: Toronto Western Hospital, Krembil Discovery Tower, 7th Floor Room 7KD402, 60 Leonard Avenue, Toronto, Ontario M5T 2S8, Canada.
E-mail address: carlen@uhnresearch.ca (P.L. Carlen).

Available online on ScienceDirect (www.sciencedirect.com).

http://dx.doi.org/10.1016/j.nbd.2015.06.005
0969-9961/

In a previous report, our group described a model of hypoglycemic seizures in the intact hippocampal preparation from mice ≤ 13 days/old (Abdelmalik et al., 2007). In that work, changing the perfused glucose concentration from 15 mM to 4 mM induced seizure-like events (SLEs) recorded in CA1 in 73% (11/15) of the preparations. However, the onset zone and the cellular mechanisms associated with the hypoglycemia-induced seizure like events (SLE) within the hippocampus were not clearly established. In this work, we used "thick" hippocampal slices from more mature animals aged 14–21 days to establish the putative area of seizure origin in the hippocampal formation and the cellular effects of low glucose perfusion in CA3 pyramidal cells.

Additionally, we describe the effects of hypoglycemia on two intrinsic rhythms observed in the thick hippocampal slice; baseline sharp-waves (bSPW) which are strongly correlated with $GABA_A$ inhibitory postsynaptic potentials (IPSPs) on CA3 pyramidal cells (Ellender et al., 2010; Hajos et al., 2013; Maier et al., 2003; Wong et al., 2005), and the large amplitude sharp waves (LASW) (El-Hayek et al., 2013; Wu et al., 2002, 2005b, 2009), a designation given to >300 μV SPW-like events associated with spontaneous increased excitatory neurotransmission and pyramidal cell firing observed spontaneously, or induced by tetanic stimulation in mouse isolated thick hippocampal slices. Here, we show that hypoglycemia depressed bSPW and enhanced LASW along with a progressive neuronal membrane depolarization and glutamate receptor activation, phenomena associated with seizure initiation in the CA3 region, often followed by spreading depression in the CA1 region.

Materials and methods

Tissue preparation

C57BL6 male mice postnatal days 14–21 from Charles River Breeding Farm (Montreal, Quebec, Canada) were used. They were housed with one to six other littermates and a nursing mother in a vivarium with a 12 h light/dark cycle at a constant 23 °C. All the procedures presented in this work were approved by the local animal care committee and followed the Canadian Council on Animal Care guidelines. From these animals, thick slices were obtained as previously described. Briefly, under general anesthesia with pentobarbital (70 mg/kg), the mice were perfused intracardially with a neuroprotective solution consisting of sucrose 248 mM, KCl 2 mM, $MgSO_4$ 3 mM, $CaCl_2$ 1 mM, $NaHCO_3$ 26 mM, NaH_2PO_4 1.25 mM, and D-glucose 10 mM followed by fast decapitation and brain removal. The brain was hemisectioned and placed into cold (~4 °C) dissecting solution containing 1 mM of kynurenic acid for 4–5 min, followed by the brain stem and thalamic tissue removal, then glued and sliced to 800 μm or 500 μm sagittal to the hippocampal axis, using a semiautomatic vibrotome (Leica VT1200), the surrounding neocortex and entorhinal cortex were removed, and finally dentate gyrus separated from CA1 and CA3 using a glass probe (Wu et al., 2005b). The recovered slices were placed into a storage chamber containing artificial cerebrospinal fluid (ACSF) made of NaCl 123 mM, KCl 3.5 mM, $CaCl_2$ 1.5 mM, $MgSO_4$ 1.6 mM, sodium bicarbonate 25 mM, NaH_2PO_4 1.2 mM, D-glucose 10 mM, osmolarity of 298 ± 7, with a pH of 7.37 ± 0.05 after bubbling with a mixture of 95% O_2 and 5% CO_2, at 34 °C for 30 min. We allowed passive cooling to room temperature (21 °C) and recovery for at least one-half hour prior to starting the recording protocol.

Electrophysiology

Recordings were carried out in a modified Haas interface chamber for extracellular field recordings as previously described by Wu et al. (2002), and a custom made submersion chamber for patch clamp experiments. Both systems use a bridge consisting of a metallic ring and a mesh on top to allow a raised placement of the tissue from the floor of the chamber, permitting the perfusion of solution (flow rate 10–15 cm^3/min) above and below the brain slice, in order to maximize the oxygen diffusion into the preparation, thereby improving the probability of observing spontaneous hippocampal rhythmic activities (Hajos et al., 2009; Wu et al., 2002). Under these conditions, only slices with a stable evoked response of ≥0.5 mV and the presence of afterdischarges after a maximum of two 1 s stimuli at 100 Hz using 70% of the amperage required to obtain the maximum amplitude of field excitatory post-synaptic potentials (fEPSPs) in CA3 and CA1 were used for the challenge protocol. To evaluate the effects of severe hypoglycemia on the CA3 bSPWs while avoiding the development of seizure-like events (SLEs), 500 μm brain slices were used. In our experience, their more limited circuitry seems to fail in generating hypoglycemia induced SLEs in submerged perfusion chambers.

Dual extracellular field recordings of either CA3 and CA1 pyramidal layers or CA3 pyramidal layer and stratum radiatum were performed using glass micropipettes (World Precision Instruments, Inc., Sarasota, FL), 1 μm tip diameter (1–2 MΩ resistance), filled with 150 NaCl solution (Abdelmalik et al., 2007). The signals were amplified by an Axopatch 200B or a MultiClamp 700B amplifier (Axon Instruments), with sampling rates of 10 kHz, low-pass filtered to 5 kHz. Field potentials were evoked by constant current stimulation of mossy fibers using a custom made bipolar stimulating electrode (0.1–0.15 ms, 40–150 μA, 1–2 per minute), eliciting maximum evoked field excitatory post-synaptic potentials (fEPSPs).

Somatic whole cell recordings under current or voltage clamp mode were obtained using patch pipettes containing (in mM) 10 NaCl, 135 K-gluconate, 1 $MgCl_2$, 10 NaHepes, 0.3 NaGTP, 2 NaATP, pH 7.25, slightly modified from McBain (1994), with a final resistance in the bath ranging from 5–7 MΩ. Only cells with a resting membrane potential (RMP) more negative than −50 mV, stable access resistance (<20 MΩ), and input resistance >100 MΩ were used for subsequent analyses. Continuous monitoring of access resistance was performed before and during the hypoglycemic challenge. Spontaneous and evoked EPSPs and IPSPs were obtained at the RMP and quantified for frequency and amplitude changes during the different experimental conditions.

Hypoglycemic challenge protocol

The challenge protocol consisted of a baseline of 15–30 min ACSF (D-glucose 10 mM) perfusion, followed by up to 30 min of severe hypoglycemia (D-glucose 1 mM), and in a subgroup of slices a subsequent 20–30 min of glucose reperfusion. In a different group of slices, rescue glucose reperfusion was started immediately if seizure-like events (SLEs) were observed at any time during the challenge. Precautions were taken to correct changes in osmolality beyond 10 mOsm between solutions by adding sucrose as needed. Finally, in a subgroup of slices, the 1 s 100 Hz stimulus above described was repeated after the first 10 to 30 min of hypoglycemia in order to evaluate the susceptibility of the circuitry for generating after discharges or SLEs.

Pharmacology

5,5-Diphenylimidazolidine-2,4-dione (phenytoin), 6-cyano-7-nitroquinoxaline-2,3-dione (CNQX), (+)-5-methyl-10,11- dihydro-5*H*-dibenzo[*a*,*d*]cyclohepten-5,10-imine maleate (MK-801), and (2*R*)-amino-5-phosphonopentanoate (AP5), (6*R*)-6-[(5*S*)-6-methyl-5,6,7,8-tetrahydro[1,3]dioxolo[4,5-*g*]isoquinolin-5-yl]furo[3,4-*e*][1,3]benzodioxol-8(6*H*)-one (Bicuculline), were acquired from Sigma-Aldrich. Stock solutions were prepared in ACSF or distilled water and diluted to the indicated concentrations for the different experiments.

Data analyses

Variables evaluated were the amplitude of field excitatory postsynaptic potentials (fEPSPs), and amplitude, frequency, and

area under the curve of the spontaneous oscillatory activity including baseline SPW (bSPW) and large amplitude sharp waves (LASW). We also addressed the presence of spontaneous or evoked seizure-like activity under severe hypoglycemia and its features. For this, off-line analyses were performed using template and threshold search modes in Clampfit 10.0 (Axon Instruments) using a minimum threshold of 2 standard deviations from the mean field potential noise level. After running the template search, recordings were visually reviewed and false-positive events were rejected from the analysis. The delay between signals recorded in CA3 and CA1 fields (general and per event) were obtained using the calculated time lag corresponding to the highest cross-correlation estimate obtained in Clampfit 10.0 (Axon Instruments) and cross-correlograms in MATLAB 2010 (MathWorks). Statistical analyses were performed using Sigmaplot 11.1 and applying the t-test, exact Fisher test, or chi-square test as required. Statistical significance was considered when p values were <0.05. Results are presented as mean ± SEM.

Results

The thick slice is a reliable preparation to model hypoglycemia-induced seizure like events (SLEs)

The standard (400–500 μm) brain or hippocampal slice has been widely used to evaluate the effects of severe hypoglycemia and aglycemia on synaptic transmission in the CNS (Calabresi et al., 1997; Crepel et al., 1992; Fan et al., 1988; Izumi et al., 1994; Kim et al., 2007; Shoji et al., 1992; Tekkok et al., 2002; Zhao et al., 1997). However, slices of this width do not display hypoglycemia-induced seizures. The thick slice preserves more of the intrinsic and recurrent circuitry of the hippocampus permitting expression of intrinsic hippocampal network activity in slices not only from ventral but also from dorsal areas (Wu et al., 2002, 2005b, 2006). The association between hippocampal intrinsic rhythms is now being extensively studied in the context of epilepsy (Beenhakker and Huguenard, 2009). Using the thick slice, we decided to evaluate the functional effects of severe hypoglycemia on the isolated DG–CA3–CA1 circuitry. Interestingly, severe glucose depletion led to one or two spontaneous ($n = 10$) or a single train-evoked ($n = 4$) seizure-like event (SLEs) in 14/16 (88%) of thick slices ($n = 14/16$, exact Fisher test; $p = 0.007$) (Figs. 1A and B). When spontaneous, these SLEs appeared after 5.3 ± 2.9 min (range: 2.5–13 min) of low glucose perfusion, with a mean duration of 44.3 ± 25 s in CA3 and 39.4 ± 23 s in CA1 (Fig. 1A). These SLEs had amplitudes of 1.85 ± 0.28 mV in CA3 and 0.57 ± 0.39 mV in CA1 (t-test; $p < 0.001$). In both subfields, the SLEs were dominated by low frequencies (4.4 ± 2.2 Hz in CA3 vs. 2.6 ± 1.3 Hz in CA1; t-test, $p = 0.549$). There were no SLEs observed during hypoglycemia in experiments using 500 μm slices ($n = 6$), however, as expected, the 500 μm slices showed interictal events under $GABA_A$ blockade with bicuculine ($n = 6$), and SLEs during low Mg/high K perfusion ($n = 5$).

Electrographically, the SLEs induced by severe glucose depletion fulfilled the criteria observed in other epilepsy models in vitro (Anderson et al., 1986; Avoli et al., 1996; Yaari et al., 1983), including the display of at least three arbitrarily defined dynamic states: preictal, with duration of 18.9 ± 5.2 s ($n = 13$) and frequency of 3.4 ± 0.7 Hz ($n = 12$), ictal, defined as high amplitude and higher frequency stereotypic activity observed following the build-up or preictal period, with a duration of 10.6 ± 1.5 s ($n = 14$) and frequency of 8.1 ± 1.0 Hz ($n = 13$), which ends in a late ictal period comprising the transition out of the seizure activity, duration 28.2 ± 6.6 s ($n = 13$) and a reduced mean frequency of 3.7 ± 0.9 Hz ($n = 13$), characterized by progressive decrease in frequency and amplitude of the ictal activity (Fig. 1B). These SLEs were prevented by the anticonvulsant, 5,5-diphenylimidazolidine-2,4-dione (phenytoin) at a clinically relevant concentration (50 μM) ($n = 5, 5/5$, Fisher exact test; $p = 0.001$) (Fig. 1C). These similarities to other seizure models indicate that severe glucose depletion is another way to trigger seizures in vitro, provided one uses a thick slice containing enough intrinsic circuitry.

Another interesting observation during severe hypoglycemia in the thick hippocampal slice is a marked extracellularly measured hyperpolarizing DC shift of 5 to 10 mV following the SLE (12/14 slices, Fig. 1D). During these DC shifts, it was not possible to evoke field potentials with electrical stimulation, in agreement with them being a spreading depression-like phenomenon (SD) (Abdelmalik et al., 2007; Footitt and Newberry, 1998). The observed synaptic failure was reversible only if glucose was restored to normal levels within the first 20 s after the SLE onset (10/12, z score 2.531, $p = 0.011$). SDs have been previously observed in different brain structures (Bures et al., 1984; Fifková and Bures, 1964) and reported as the in vitro correlate of cortical spreading depression observed in EEG from patients with stroke, migraine aura and seizures (Lauritzen et al., 2011; Smith et al., 2006). SDs are believed to represent a broad depolarization of neurons, often associated with a marked increase in extracellular potassium (Smith et al., 2006) and increased glutamate release from activation of presynaptic NMDA receptors (Zhou et al., 2013). We observed SDs in 12/14 thick slices after SLEs (Fig. 1D), eight originating in CA1 and four in CA3 (Fisher exact test; $p \leq 0.05$). No SDs were recorded in control conditions ($n = 10$). Simultaneous CA3 and CA1 recordings with the distance between electrodes of 2 mm ($n = 6$ CA1 originating SD-like events), showed that the propagation speed from CA1 to CA3 was ~1.5 mm/min (Fig. 1D).

Effects of severe hypoglycemia on hippocampal rhythmic activity

The thick slice permits the expression of two different intrinsic rhythms; the GABA correlated baseline SPW (bSPW), and the glutamate-dependent large amplitude sharp wave (LASW) (Fig. 2). Both of these activities were observed to be initiated in the CA3 subfield by direct observation of the signal delay as previously described (Wu et al., 2005a,c). Given the above described epileptogenic nature of severe glucose depletion in this preparation, we wanted to evaluate the effects of severe hypoglycemia on these intrinsic hippocampal rhythms and their role in the transition to seizure during severe hypoglycemia. We observed that all SLEs induced by severe glucose depletion were preceded by one or more LASWs ($n = 14$ slices) (Fig. 3A). Additionally, in six thick slices where self-sustained LASWs were evoked by one or two trains of 100 Hz stimuli during perfusion of normal ACSF (Behrens et al., 2005), subsequent severe hypoglycemia decreased their inter-event interval (IEI) and increased their area under the curve (IEI 12.8 ± 0.7 vs. 8.6 ± 0.4 s, $p \leq 0.001$, and area 18.4 ± 1.1 vs. 23.2 ± 1.6 mV * ms, $p = 0.027$, $n = 62$ events from 6 slices) (Fig. 3B). These LASWs progressively changed their morphology merging into electrographically discernible pre-ictal events denoted by the presence of 2–6 biphasic potentials (Anderson et al., 1986) and non-significant increases in the ripple frequency from 91.8 ± 32 to 143.6 ± 84.7 Hz (Fig. 3C; $n = 6$ slices). In a subgroup of tissues, LASWs were evoked only transiently by one or two one-second trains 100 Hz. In these tissues, later exposure to severe hypoglycemia was able to induce LASWs (7/14 thick slices; Fig. 3D). Spontaneous, evoked and hypoglycemia-induced LASWs were all associated with bursts of action potentials measured in CA3 pyramidal cells ($n = 7$) and putative interneurons ($n = 3$) (Fig. 3E). LASWs originate in CA3, depend on glutamatergic receptor activation and are resistant to $GABA_A$ receptor blockade with bicuculline (Wu et al., 2005b, 2009). These findings indicate progressive CA3 neuronal recruitment during severe glucose depletion prior to seizure onset.

Evaluating the evoked extracellular synaptic potentials during severe glucose depletion, it was noted that the CA3 area was less susceptible than CA1 to developing synaptic depression ($n = 6$, CA1 fEPSP dropped from 0.89 ± 0.18 to 0.57 ± 0.16 mV, $p = 0.006$ vs. CA3 from 1.06 ± 0.4 to 0.99 ± 0.4 mV, $p = 0.663$, Fig. 4A), a phenomenon previously described during hypoglycemia in standard brain slices

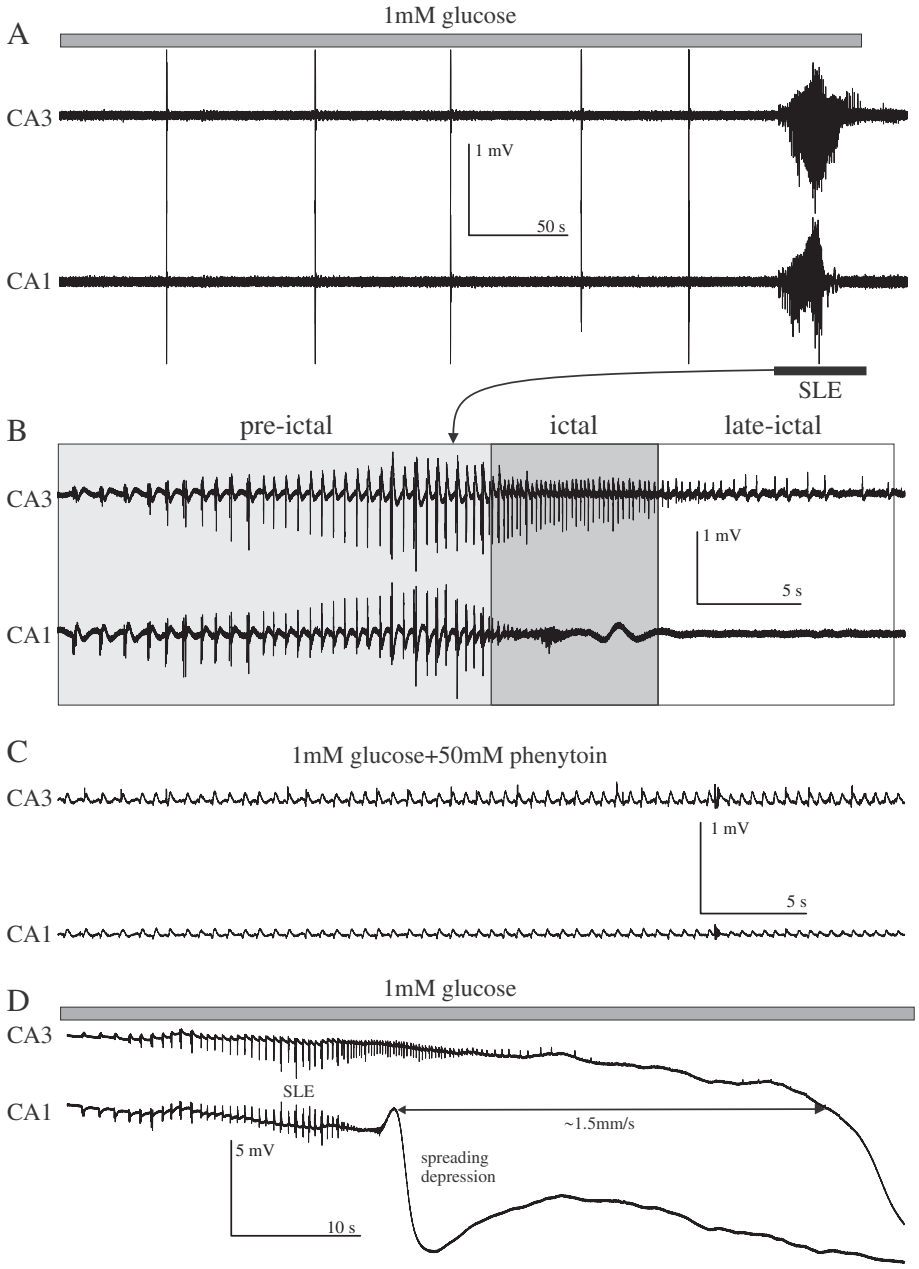

Fig. 1. Low glucose perfusion induces epileptiform activity in the thick slice. A. Representative trace showing SLE observed after ~5 min of glucose depletion in the thick slice. Top trace is the signal from CA3 and bottom trace from CA1. B. Faster sweep of the SLE in A showing that low glucose induced SLEs display different dynamic states, pre-ictal, ictal and late-ictal. C. Representative trace of severe glucose depletion and 50 μM phenytoin showing the prevention of hypoglycemia-induced SLEs (n = 5 slices). D. Representative trace of SLE induced by low glucose perfusion associated with SD-like activity initiated in CA1 spreading to CA3 at a speed of ~1.5 mm/s.

using monosynaptic stimulation of mossy fibers and Schaffer collaterals (Crepel et al., 1992). We observed that during the hypoglycemic challenge, not only were evoked potentials following a single stimulus not significantly depressed in the CA3 region in thick slices, but rather the same stimulus displayed a higher probability of evoking ripple activity (4 to 15 small population spikes following a single stimulus) or a LASW capable of spreading to the CA1 area (n = 5 slices each group; 3/5 hypoglycemia vs. 0/5 control, Fig. 4B).

In our hands 10/16 thick slices displayed baseline sharp waves (bSPW) in control conditions (62.5%). Similarly to LASW, bSPWs originate in CA3 and spread to CA1; however, this rhythm is strongly correlated with $GABA_A$ receptor activation (Ellender et al., 2010; Hajos et al., 2013; Wu et al., 2006). Examining the effects of hypoglycemia on bSPWs, we observed an initial increase in frequency (1.6 ± 1 Hz vs. 3.06 ± 3 Hz, $p < 0.001$) and amplitude (28.9 ± 1 μV vs. 36 ± 1 μV, $p = 0.001$) with increased variability in their inter-event interval (n = 7). This pattern was sometimes (3/7 thick slices) followed by bSPW disappearance, being replaced by isolated short duration (<20 ms), small amplitude (20–50 μV), fast frequency activity similar to ripple activity and multiunit activity measured in the somatic layer of CA3. This was also observed during glucose depletion in standard brain slices (500 μm) (n = 6), which are capable of displaying bSPWs under high perfusion flow rate (Hajos et al., 2009). Similar phenomenon was recently reported by Karlocai et al. (2014) in different seizure models (Karlocai et al., 2014). Furthermore, $GABA_A$ blockade with 10 μM bicuculline in this preparation replicated this finding (n = 6) (Fig. 4C). As expected, none of the thinner standard slices showed hypoglycemia-induced SLEs. Changes in bSPWs happened 90 ± 48 s (n = 7 slices) prior to SLE onset in the case of glucose depletion in thick slices and 49 ± 30 s in the case of SLE onset induced by bicuculline in standard slices (n = 6 slices). A final indication of the

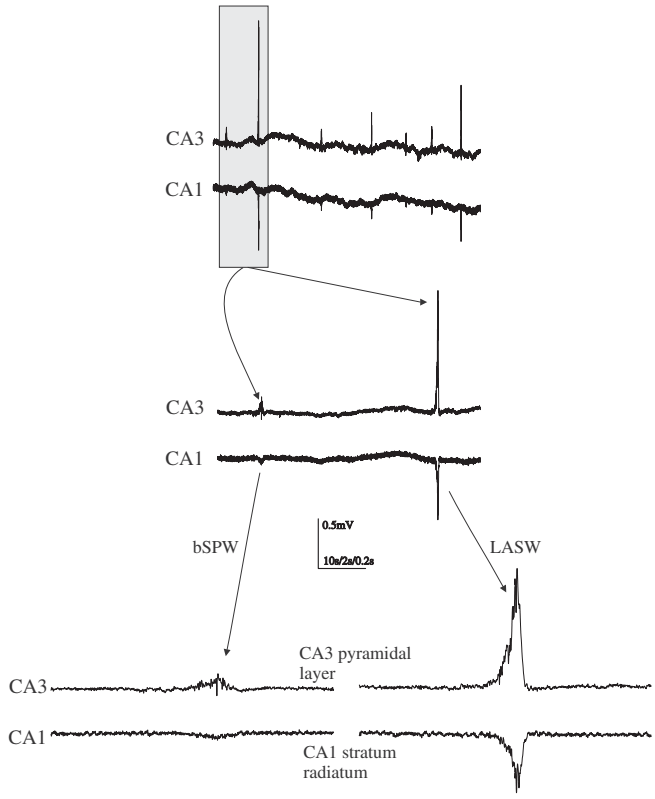

Fig. 2. Representative traces of baseline sharp wave (bSPW) and large amplitude sharp wave (LASW) occurring in a thick hippocampal slice after two tetanic stimulations.

excitation/inhibition imbalance induced by severe hypoglycemia was the change in response observed during mossy fiber tetanic stimulation (100 Hz for 1 s), which, under hypoglycemia, elicited enhanced after-discharges or full seizures (Fig. 4D).

All the above indicates that severe glucose depletion induces profound changes in the hippocampal intrinsic rhythms, more apparent and often starting in the CA3 region prior to the onset of SLEs. Shortly after the initiation of the challenge, there is a transient increase in bSPW activity, reflecting enhanced GABAergic interneuronal network activity in CA3, probably due to increased GABA release shown to be present under different pathophysiological conditions such as hypoxia, hypoglycemia, ischemia and oxidative stress (Gee et al., 2010; Saransaari and Oja, 1997). However, if the challenge continues, this transient enhancement could be replaced by relative GABAergic synaptic failure, as seen in other epilepsy models (Karlocai et al., 2014; Zhang et al., 2012), and demonstrated by the disappearance of bSPWs. Additionally, there appears to be progressive neuronal recruitment, indicated by the enhancement of after-discharges and the higher probability of expression of LASWs or the development of pre-ictal events from LASWs. This recruitment could be dependent on the subsequent increase in the excitatory drive in CA3, both factors possibly leading to the imbalance between inhibition and excitation resulting in the preictal and ictal activity.

CA3 is the area of onset of hypoglycemia-induced seizures in the "thick" hippocampal slice

As mentioned previously, the hypoglycemia-induced SLEs were all preceded by one or more spontaneous LASWs (n = 14 slices), and there was an observable delay between CA3 and CA1 preictal bursts signals (Fig. 3D, 5A). These initial observations suggested us that the seizure onset during severe glucose depletion in the hippocampus is in the CA3 area. More objectively, calculation of the delay time of each hypoglycemia-induced SLE quantified as the time lag between signals corresponding to the highest peak on the cross-correlation estimate between CA3 and CA1 signals, showed that the SLEs recorded in CA3 led the SLEs recorded in CA1 by 19.8 ± 6.9 ms (n = 8 SLEs). However, this quantification reflects summation of delays in the signal of all the bursting events part of SLEs, leaving the possibility that the onset zone of hypoglycemia-induced SLEs could be from either the CA3 or CA1 regions. Thus, a more specific quantification is to evaluate the delay time between individual pre-ictal bursting events of hypoglycemia-induced seizures between both areas using cross-correlation analysis between CA3 and CA1 signals. This quantification showed that during the pre-ictal phase, individual events more commonly originated in the CA3 region (47/66 events in 6 slices, 71%, chi-square p = <0.001), leading the CA1 signal on average by 27.3 ± 5.6 ms (n = 66 pre-ictal events). However, 19/66 events classified as pre-ictal started in CA1, indicating the possibility that pre-ictal events, although usually originating in CA3, as the phenomenon progresses there is dynamic interaction between CA3 and CA1, as expected for a coupled oscillatory system (Derchansky et al., 2006). This evaluation was corroborated by cross-correlogram analyses run in a subset of traces which also showed higher estimates in the signal originated from the CA3 region ($n = 6, p < 0.001$) for individual pre-ictal events and a then a shift towards cross-talking between CA3 and CA1 as the system approached the time of the ictus. This oscillatory shifting of burst onset region between CA3 and CA1 continued during the ictus (Figs. 5B and C).

The signal delay analysis is a good method to postulate putative origin of electrographic events, however, it does not completely rule out DG, CA1 or CA3 as area of onset of the SLEs observed during severe hypoglycemia in our recordings. To finally confirm that CA3 circuitry was indeed the zone of origin for hypoglycemia-induced seizures, we disconnected the mossy fibers or Shaffer collaterals, and recorded during glucose depletion from different areas of the thick slice (Fig. 5D). Initially, we evaluated the role played by the DG input into the CA3 region in the induction of hypoglycemic SLEs by cutting the mossy fibers and performing recordings in DG and CA3. These experiments showed that without the DG input, the CA3 circuitry is still capable of displaying epileptiform activity induced by severe hypoglycemia (4 of 4 slices, n = 4). Although the induced SLEs were smaller in amplitude and shorter in duration, similar results were obtained when Schaffer collaterals from CA3 to CA1 were cut (4 of 4 slices, n = 4), ruling out CA1 onset and back-propagation spreading to CA3, but indicating its important role for further enhancement of the SLEs initiated in CA3, also in agreement with a prior report of CA3–CA1 functioning as coupled oscillator system during seizure activity (Derchansky et al., 2006). In another set of experiments, removing the CA3 and DG areas from the thick slice while recording from the intact CA1 and subiculum, prevented the expression of hypoglycemic seizures in the isolated CA1 region (0 of 4 slices, n = 4). Finally, preparation of the CA3 region into a mini-slice (tissue containing only the intrinsic CA3 circuitry), demonstrated that the CA3 region was able to exhibit robust seizure activity under severe hypoglycemia without any additional input from other adjacent areas (4 of 5 slices, n = 5). In conclusion, these experiments showed that the CA3 circuitry is the area of seizure generation in the hippocampus under severe glucose depletion.

CA3 pyramidal cells depolarize during severe hypoglycemia

CA3 pyramidal cells (AP duration of ≥1 ms and generation of burst of APs) had resting membrane potentials (RMP) of −64.37 ± 2.3 mV, input resistances (IR) of 142.73 ± 17 MΩ and maximum firing frequencies of up to 43 ± 7 Hz (n = 8). During severe hypoglycemia, these cells showed a significant decrease in input resistance measure from repeated I/V curves prior and after hypoglycemia (from 142.73 ± 17 MΩ to 110.2 ± 12 MΩ, paired t-test; p = 0.029) (Fig. 6A). Additionally, observation of the membrane potential displayed by CA3 pyramidal cells during severe glucose depletion showed a short transient hyperpolarization followed by a significant

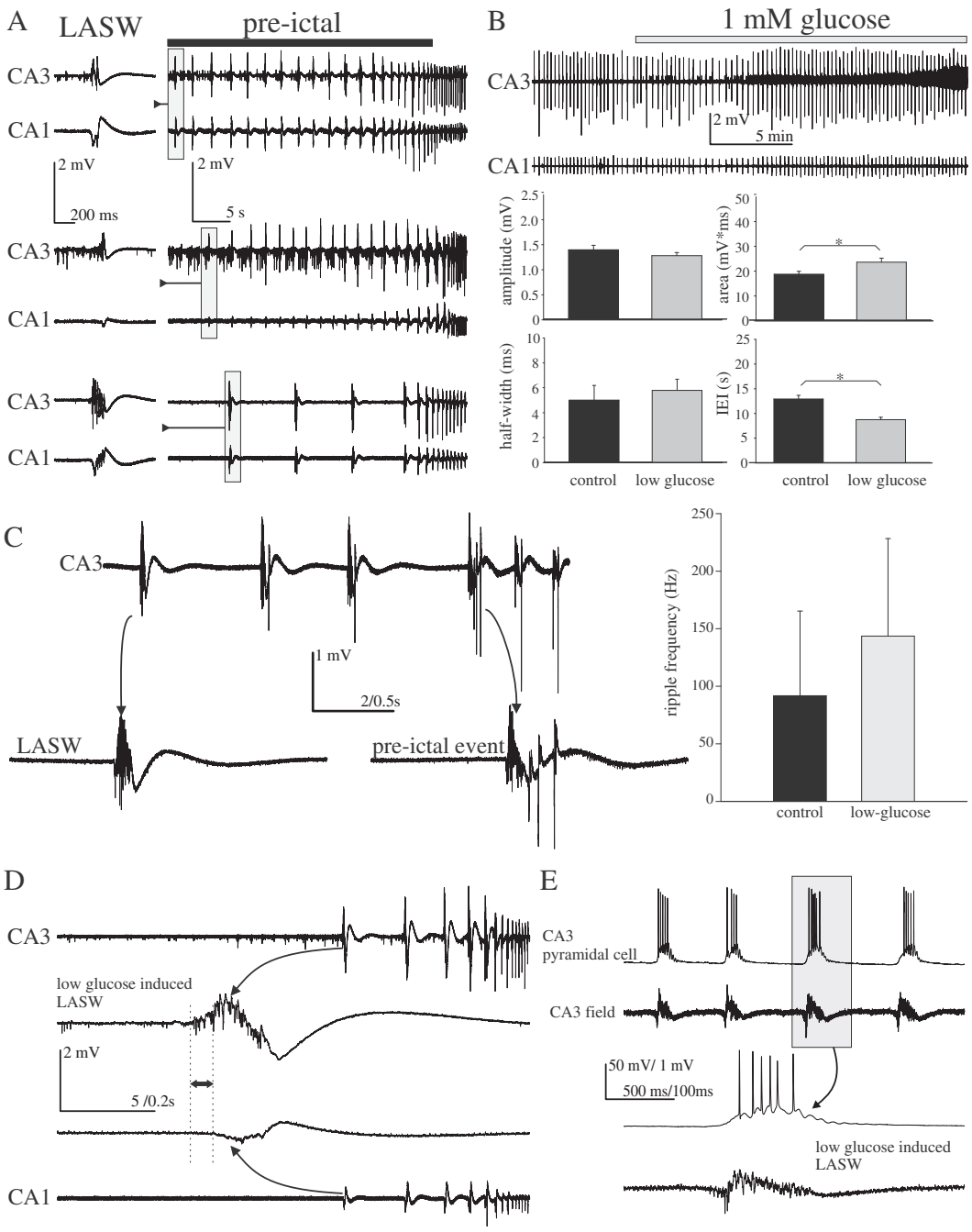

Fig. 3. Effect of low glucose perfusion on CA3 LASWs. A. Representative traces from 3 thick slices showing CA3 LASWs preceding low glucose SLEs. B. Top, representative trace of the effects of low glucose perfusion on CA3 originated LASWs. Bottom, bar graphs of effect of low glucose on amplitude, area under the curve, half width and inter-event interval (IEI) of CA3 LASWs ($n = 62$ events from 6 slices). C. Left, representative trace showing the transformation of CA3 LASWs into pre-ictal events. Right, bar graph comparing the mean ripple frequency of CA3 LASWs prior to and following the onset of SLEs. D. Representative trace showing CA3 to CA1 LASWs induced by low glucose perfusion prior to the onset of SLEs. E. The intracellular correlate of CA3 LASWs induced by low glucose perfusion. Note the depolarization of the CA3 pyramidal cell and the bursting of action potentials shown in phase with the CA3 LASWs.

progressive slow depolarization (from -64.17 ± 1.3 to -58.20 ± 2.4 mV, 7/8 CA3 pyramidal cells, Fig. 6B) which was resistant to synaptic blockade induced by ACSF containing 3 mM Mg^{2+} and 0.5 mM Ca^{2+} (from -63.89 ± 23 to -57.86 mV, 5 of 6 pyramidal cells, $n = 6$). Prior to the hypoglycemia induced SLEs, the slow depolarization was associated with increase in the area (64.3 ± 2.6 vs 73.2 ± 1.9 mV $*$ ms, $p = 0.006$), rise (11.1 ± 0.3 vs 13.6 ± 0.4 ms, $p \leq 0.001$) and decay time (21.03 ± 0.4 vs 22.2 ± 0.3 ms) of spontaneous EPSPs, while the IPSPs (reversal potential approximately -55 mV) recorded in CA3 pyramidal cells were progressively decreased in amplitude and area (1.45 ± 0.07 vs 1.35 ± 0.03 mV and 57.2 ± 4.7 vs. 38.8 ± 1.9 mV $*$ ms, t-test $p \leq 0.001$) (Fig. 6C). These findings agree with the concept of initial increase in tonic inhibitory activity during glucose depletion, manifested as the transient membrane hyperpolarization observed in pyramidal cells and previously described in standard preparations (Knopfel et al., 1990; Spuler et al., 1988), with a transient increase in the frequency of bSPW activity, which is then replaced by increase excitatory drive in CA3 prior to the seizure (see section: effects of severe hypoglycemia on hippocampal rhythmic activity).

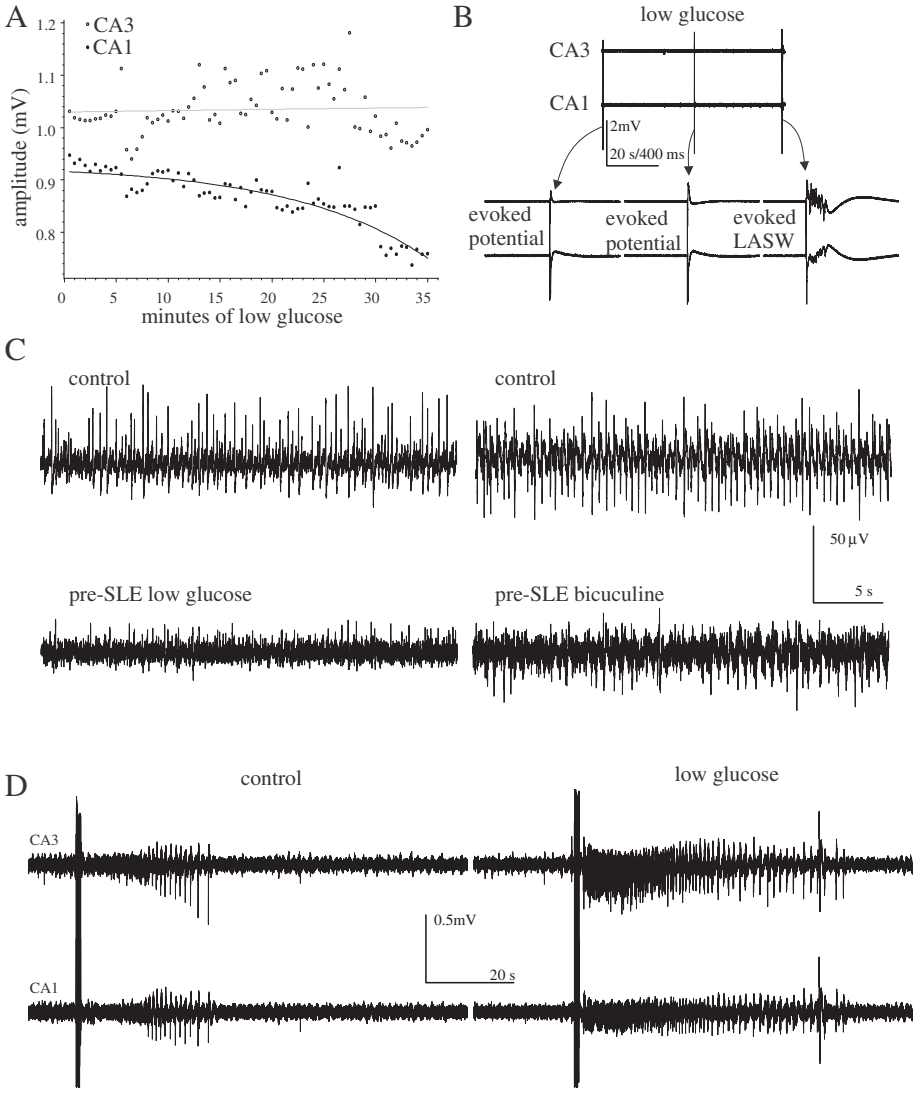

Fig. 4. Effect of low glucose perfusion on CA3 circuitry. A. Scatter plot showing the change in amplitude over time of low glucose perfusion on the mossy fiber stimulation evoked field synaptic potentials recorded in CA3 and CA1 in a 600 µm slice. B. Low glucose perfusion in thick slices is capable of inducing evoked LASWs in CA3 and CA1. C. Low glucose perfusion effects on CA3 GABA-dependent bSPWs. A similar pattern was reproduced by application of the GABAA receptor blocker bicuculline (10 µM). D. Representative trace of 100 Hz/1 s mossy fiber stimulation after discharge response induced in CA3 and CA1 before and after low glucose perfusion in the thick slice.

Role of glutamatergic transmission in hypoglycemia induced-SLEs and SD

Previous work on insulin-induced hypoglycemia in vivo consistently found increases in GABA, glutamate and aspartate brain content (Sandberg et al., 1986). Glutamate excitatory action in the hippocampus is due to its binding to the AMPA, NMDA, and kainate receptors. The mossy fibers synapsing onto CA3 pyramidal cells activate mainly AMPA postsynaptic receptors (Jonas et al., 1993; Monaghan et al., 1983); however, the changes in EPSPs and the progressive depolarization suggest activation of both fast and slow glutamatergic receptors. There is evidence linking NMDA receptor activation and the cytotoxicity associated with severe hypoglycemia (Facci, Leon, & Skaper, 1990; Ichord et al., 2001). Thus, we decided to evaluate the role of specific postsynaptic glutamatergic activation on the actions of hypoglycemia in thick slices. Perfusion with the AMPA/kainate receptor blocker, CNQX (20 µm) prevented the development of hypoglycemia-induced SLEs and SDs (Figs. 6A and C), and the production of LASWs (4 of 4 slices, n = 4). Interestingly, these effects were also observed when we applied the noncompetitive NMDA receptor blocker MK-801 (50 µM) via the perfusate 10 min before and during severe hypoglycemia. In these experiments (n = 5), no slice demonstrated well-defined SLEs (exact Fisher test, p = 0.001, Fig. 7A), and the transformation of CA3 LASWs into pre-ictal events was prevented in seven slices that presented LASWs after one or two trains of stimulations (58 control events; amplitude 2.65 ± 0.6 mV, frequency 0.27 ± 0.11 Hz, area 87.52 ± 51 mV ∗ ms, half-width 16.6 ± 7 ms, vs. 126 hypoglycemia + 50 µM APV events; amplitude 2.6 ± 0.4 mV, frequency 0.42 ± 2 Hz, area 63.1 ± 31 mV ∗ ms, half-width 10.9 ± 4.3 ms, t-test: p < 0,05. Fig. 6B). However, when we applied MK-801 (50 µM) or the competitive blocker APV (50 µM) at the onset of severe glucose depletion, we were able only to prevent SLEs in 50% of the slices (n = 10, 5 of 10 slices). These observations indicate that severe hypoglycemia produces increased CA3-originating hippocampal network excitability dependent on NMDA and AMPA/kainate receptors, but once the network is activated, the ensuing SLEs are only partially susceptible to NMDA receptor blockade (see Fig. 7).

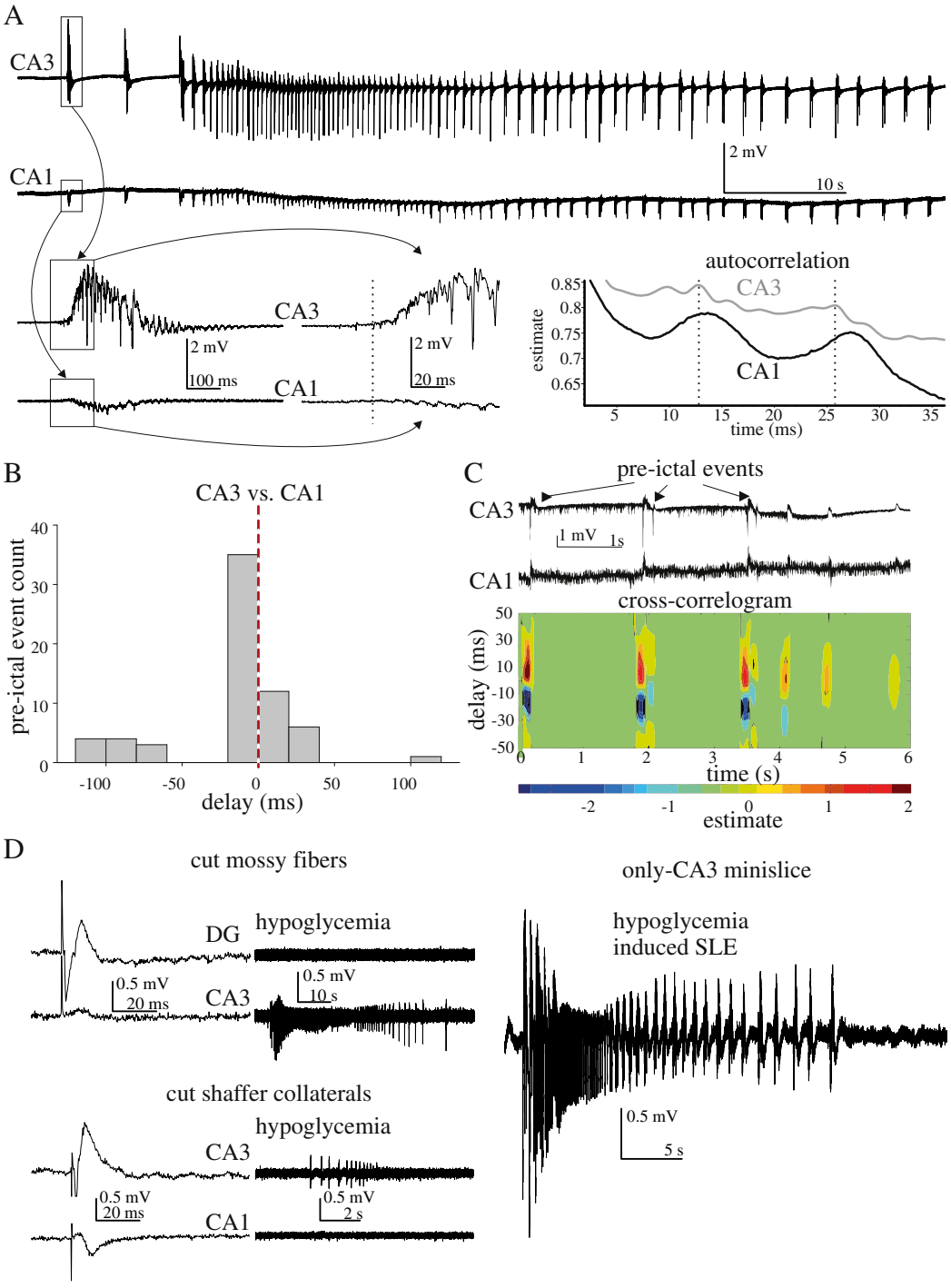

Fig. 5. SLEs induced by low glucose in the hippocampus start in the CA3 area. A. Representative trace of a hypoglycemia induced SLE in the hippocampus. Extracellular recordings from CA3 (top) and CA1 (bottom), faster sweeps of late preictal events to demonstrate presence of delay between signals. To the right, autocorrelation between the signal obtained in CA3 (gray) and CA1 (black) demonstrate higher estimates in CA3 and a signal delay in the estimate in CA1. B. Distribution of time delay between CA3 and CA1 signals taken from the highest point of cross-correlation of 66 pre-ictal events from 6 thick slices during severe glucose depletion prior to the fast frequency phase of the ictus (pre-ictal period) C. Representative trace (top) and cross-correlogram (bottom) of pre-ictal events from an SLE induced by glucose depletion showing increased correlation estimate at positive delays (CA3 signal) D. Top, DG–CA3 recordings with mossy fiber stimulation showing CA3 SLE induced by glucose depletion in a slice where mossy fibers were cut. Bottom, CA3–CA1 showing CA3 SLE recording induced by glucose depletion in a slice where Shaffer collaterals were cut. Right, representative trace from a mini-slice containing only CA3 where severe hypoglycemia was able to induce seizures.

Discussion

Seizures induced by severe hypoglycemia and the problem of recurrent neuroglycopenia

The treatment of diabetes mellitus with insulin started more than nine decades ago, and since then, hypoglycemia, severe neuroglycopenia, hypoglycemia-induced seizures and hypoglycemic coma have been described as the most serious side effects (Banting et al., 1922; Gibbs and Murray, 1954; Sakel, 1938; Tokizane, 1957). Recurrent hypoglycemia diminishes the awareness of diabetic patients for new more profound hypoglycemic events, which put them at risk of these severe complications (Ovalle et al., 1998). In clinical studies, intensive glycemic control in diabetic patients has been associated with increased

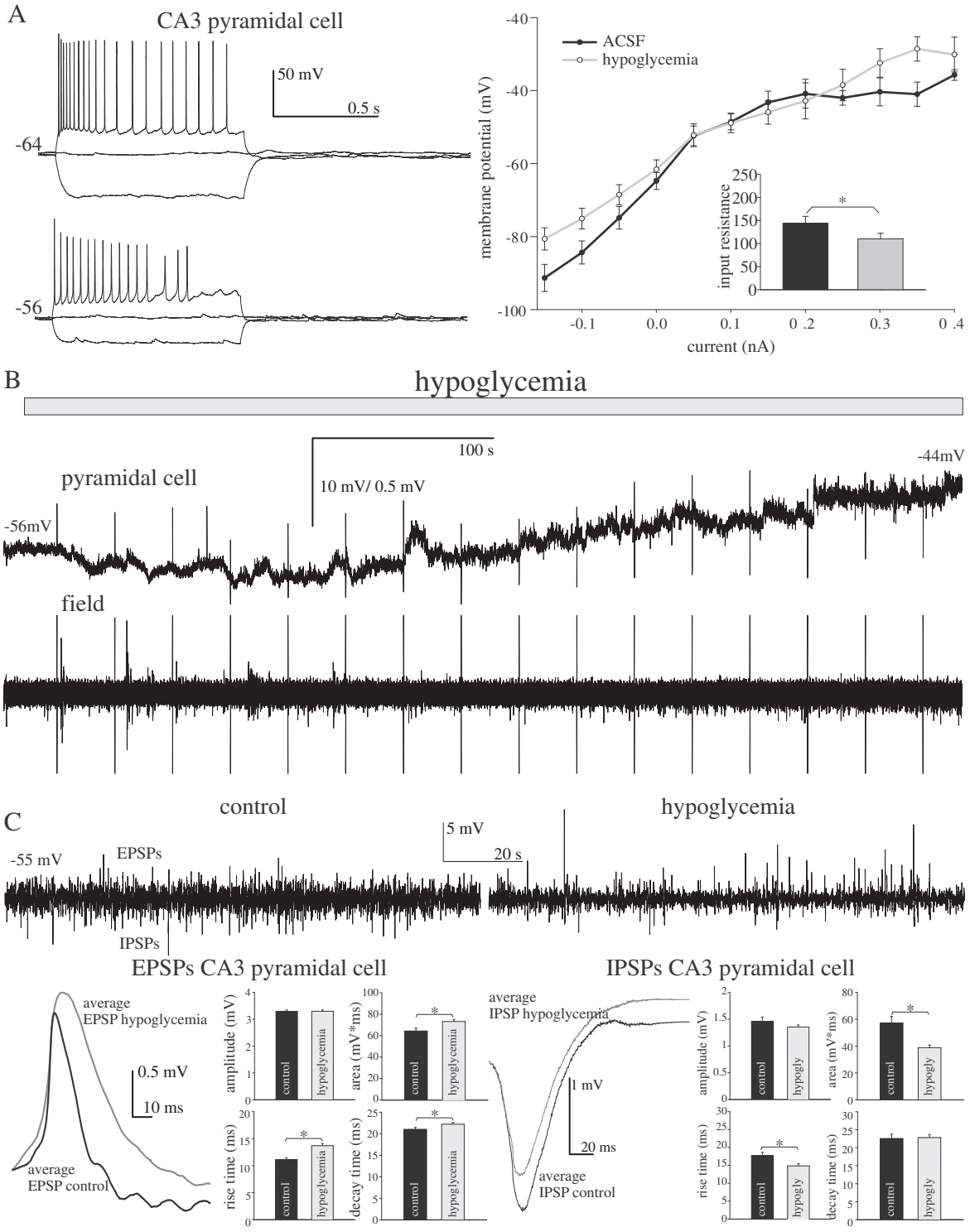

Fig. 6. Effect of low glucose on CA3 cells. A. right, representative I/V trace of a CA3 pyramidal cell in control and after 30 min of low glucose perfusion. Left, traces of membrane potential changes with intracellular injections of constant current square pulses to measure input resistance in a CA3 pyramidal cell in control and hypoglycemic conditions. Inset is the bar graph showing the calculated input resistance in both conditions (n = 8). B. Representative trace of the membrane potential of a CA3 pyramidal cell during hypoglycemia and the subsequent field recording during the initial 6 min of severe hypoglycemia. C. Top, the spontaneous synaptic activity from a CA3 pyramidal cell at resting membrane potential (−55 mV) in control conditions (right) and severe glucose depletion (left). Bottom, average EPSPs (right) and IPSPs (left) and waveform parameters during control and severe glucose depletion (n = 5).

mortality (Anon, 1994; Anon, 1997; Fanelli et al., 2004; MacLeod et al., 1993) and in ICU patients, severe hypoglycemia is an independent risk factor for worse prognosis (Lacherade et al., 2009).

The mechanisms of how severe glucose depletion leads to seizures and brain failure are not well understood. This delay is partly due to the lack of in vitro preparations showing the electrographic changes induced by severe hypoglycemia leading to seizures. It is known that the hippocampal formation is highly susceptible to low glucose (Auer et al., 1985b; Haces et al., 2010), and given its well-known morphology, physiology and biochemistry, it is reasonable to use it as a model to study the effects of severe glucose depletion in the CNS.

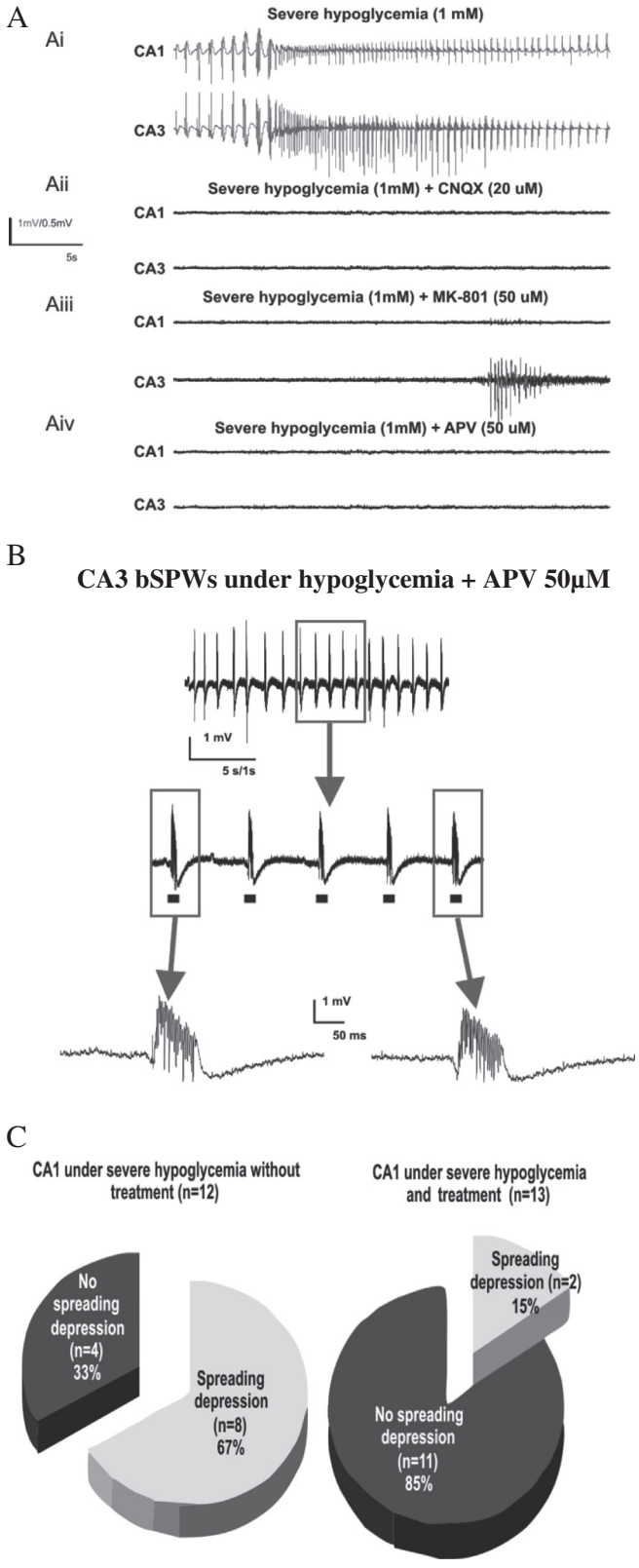

Fig. 7. Glutamate receptor blockade effect on hypoglycemia induced CA3 excitability. A. Hypoglycemic seizures are prevented by pretreatment with glutamate receptor blockers. Ai. Hypoglycemia-induced SLE, Aii. Pre-treatment with the AMPA/kainate receptor blocker CNQX (4/4 slices), Aiii, 50 µm MK-801 (5/5) and Aiv, 50 µm APV (5/5). B. Representative trace of spontaneous bSPWs under hypoglycemia and pre-treatment with APV 50 µM (n = 7 slices). C. Pie graphs showing the significant effect of NMDA receptor blockade (APV or MK-801) on the hypoglycemia induced SD. No treatment (left) and with NMDA receptor blockade (right).

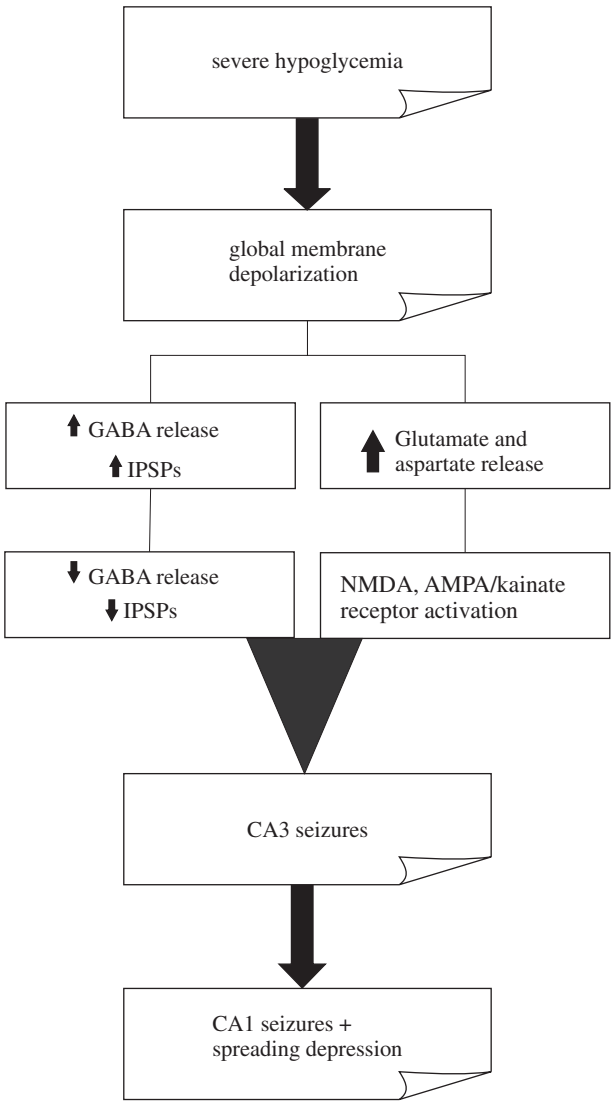

Fig. 8. Proposed mechanism for hypoglycemia-induced seizures and SD in the mouse hippocampus.

Inhibition and excitation in the hippocampus during severe glucose depletion

We evaluated the effects of severe hypoglycemia in the mouse thick hippocampal slice, a preparation used to study intrinsic hippocampal network activities (Wu et al., 2002, 2005b). SLEs were even more reliably induced by severe hypoglycemia (14 of 16 slices, 88%) in this preparation when compared to our previous study using the mouse intact hippocampus (Abdelmalik et al., 2007). However, in this work the glucose concentration in the perfusate was reduced to 1 mM, a difference that could have account for the higher success rate. It is also important to note possible differences in oxygen pressure in the middle and deep layers of the thick slice, which could account for a higher susceptibility for excitation. However, other authors (Chiovini et al., 2010; Wu et al., 2005b) have previously proved that a fast perfusion rate and appropriate tissue preparation methods decreased this possibility. Different than the whole hippocampus, the thick slice can be used in aging, diabetic, and recurrent hypoglycemic animal models, which will allow future enquires in the pathophysiology of hypoglycemic seizures under these clinically relevant situations.

During low glucose perfusion, the CA3 hippocampal rhythmic activity was affected early. We describe the effects on two intrinsic rhythms, bSPW and LASW (Wu et al., 2005b). The former type increased in frequency and area until becoming multiphasic preictal potentials in CA3 preceding the SLEs. Similar findings can be observed in the low Mg^{2+} model of epilepsy (Anderson et al., 1986), possibly due to similar mechanisms. The cause of these hyperexcitable changes could be increased glutamate and aspartate release from neuronal and non-neuronal sources and possible failure of astrocytic glutamate uptake as previously demonstrated during severe hypoglycemia, leading to excitatory receptor activation (Bakken et al., 1998; Butcher et al., 1987; Rao et al., 2010).

LASWs has been correlated with the firing of multiple neuronal populations (Wu et al., 2005b) and its enhancement might indicate increased neuronal recruitment in the CA3 area probably associated with the progressive membrane depolarization observed in pyramidal cells during severe hypoglycemia.

The bSPWs showed transient increase in frequency and amplitude followed by a decrease in rhythmicity and disappearance. In both standard and thick slices bSPWs disappear when the $GABA_A$ receptor is blocked with bicuculline (Wong et al., 2005; Wu et al., 2005b, 2006). We hypothesize that the initial transient increase in bSPW activity during low glucose perfusion is due to an unsustained increase in GABA release from the presynaptic terminal (Tossman et al., 1985), while the ensuing decrease in bSPW could be explained through several mechanisms including presynaptic GABA depletion (Huberfeld et al., 2011; Zhang et al., 2012), increased GABA uptake and catabolism, postsynaptic receptor malfunction or simply due to shift of the Cl-reversal potential (Karlocai et al., 2014; Leinekugel et al., 1999) associated with the progressive depolarization induced by hypoglycemia. There is evidence of decreased inhibitory modulation of the CA3 pyramidal cell network during hypoglycemia (Loracher and Lux, 1974; Sherin et al., 2012), however, further studies are required to clarify the role of these mechanisms in the pathophysiology of hypoglycemia induced seizures.

Slow depolarization and hypoglycemic seizure initiation

This phenomenon could be explained by early and progressive potassium accumulation in the extracellular space as demonstrated by previous animal studies in vivo during severe glucose depletion (Astrup and Norberg, 1976; Sieber et al., 1993; Wieloch et al., 1984), or to progressive activation of glutamate receptors (Semyanov and Godukhin, 2001) prior to seizure onset. In this work, we observed that NMDA and AMPA/kainate receptor activation played important roles for the recruitment of CA3 pyramidal cells into well-organized SLEs. Blocking AMPA/kainate or NMDA receptors prevented the development of synaptic failure in both CA1 and CA3 during severe hypoglycemia. In our recordings, the SLEs were followed by SDs (Smith et al., 2006), a well-documented phenomena associated with extracellular K+ accumulation and synaptic failure (Somjen et al., 1992), and reproduced in different CNS structures in vitro by N-methyl D-aspartate perfusion or other challenges associated to strong NMDA receptor activation (Basarsky et al., 1999; Kager et al., 2002; Lauritzen et al., 1988; Marrannes et al., 1988; Sheardown, 1993; Somjen, 2001). NMDA receptor activation requires the removal of a concentration and voltage dependent blockade by Mg^{2+} in the NR2 subunit (Mayer et al., 1992), which reinforces the idea that potassium accumulation could represent the early phenomena linking NMDA receptor activation, seizures, brain failure and finally cell death during severe hypoglycemia.

Having this in mind, we suggest that synaptic independent K^+ accumulation during severe glucose depletion could contribute to the development of hypoglycemia-induced SLEs. However, if this potassium accumulation is caused by fast failure of astrocytic K^+ uptake and buffering mechanisms, opening of connexin hemichannels or pannexin channels, activity dependent K^+ extrusion from the intracellular space, or a combination of these factors also remains to be elucidated. Other pathogenic factors related to hypoglycemia include increased production of reactive oxygen species, Na/K^+ ATPase pump failure, cell and nuclear membrane disruption and cell death (Isaev et al., 2007), all of which could contribute to the findings of this study, but at this time were not the focus of our scrutiny.

Regional susceptibility and its relationship with brain failure and neuronal death during severe glucose depletion

GABA and glutamate content in brain tissue recovered from severe hypoglycemic animals is increased three to six-fold when compared to controls whereas aspartate is increased to 15-fold its control levels (Sandberg et al., 1986). Aspartate accumulation has been implicated for decades in the pathophysiology of hypoglycemic brain damage. This effect is believed to reside in increased excitotoxicity induced by excessive intracellular Ca^{2+} accumulation and the activation of NMDA receptors (Ichord et al., 2001; Nellgard and Wieloch, 1992). In fact, several studies in vivo and in vitro have effectively prevented hypoglycemic neuronal degeneration and death by blocking these receptors (Papagapiou and Auer, 1990; Wieloch, 1985). Thus, there is evidence of a link between NMDA receptor activation, brain failure and cell death.

Regional differences associated with dissimilar receptor expression are noticed in systemic kainate injection showing more prominent degeneration in CA3 than CA1(Wuerthele et al., 1978). Although rat strain dependent, under kainic acid stimulation in vitro, Wistar rats CA3 is 10 fold more vulnerable than CA1 to have depolarization block (Westbrook and Lothman, 1983). This distribution is clearly different from those reported in different rodent species after severe sustained hypoglycemia, but similarly to hypoglycemia, kainic acid perfused at minimal concentrations induces SLEs starting in CA3 spreading to CA1. Unfortunately, these fundamental differences prevent us from making a parallel comparison between these two challenges.

We propose that during severe hypoglycemia, areas of the brain that are less susceptible to brain damage, such as hippocampal CA3 or deep cortical layers (layers V–VI), are more likely to display seizures, spreading to adjacent areas which are more susceptible to energy failure leading to secondary excitotoxicity. If accurate, this model would also explain the difference in the distribution of damage associated with ischemia compared to severe glucose depletion (Auer, 2004).

We suggest that the CA1 increased susceptibility to SD and synaptic failure with hypoglycemia is likely related to the inherent higher expression of NMDA receptors in the postsynaptic densities and extrasynaptic membrane of the CA1 cells as compared to CA3 cells (Butler et al., 2010; Stanika et al., 2010; Tasker et al., 1992). This "excess" of NMDA receptors is activated by the hypoglycemic-mediated increase in glutamate and aspartate (Sandberg et al., 1986). The CA1 region would display faster failure in its compensatory mechanisms mainly due to increased intracellular Ca^{2+}, aggravated by known morphological differences including its lower cell size, higher cellular compactness and decreased extracellular space (Crepel et al., 1992).

It is important to note that the effects of severe hypoglycemia on K^+ uptake and buffering mechanism in the hippocampus are unknown. These include astrocyte Na^{2+}–K^+ ATPase, Na^{2+}–K^+–Cl^- co-transporters or astrocytic inward rectifying potassium (Kir) channel activity (Kofuji and Newman, 2004). We consider that their dysfunction or regional differences in their expression might also play a role in producing the slow membrane depolarization, and the difference between CA1 and CA3 susceptibility for synaptic failure during severe hypoglycemia.

We propose the following hypothesis for the mechanisms implicated in the induction of hypoglycemic seizures, explaining the different phenomena described in vitro, and the discrepancies observed in vivo: Hypoglycemia induces increased accumulation of

extracellular potassium (Arieff et al., 1974; Carey et al., 1981), accompanied by massive release of aspartate and glutamate, and transiently GABA, which moves the balance of the circuitry towards excitation and global neuronal/non-neuronal cell activation inducing more accumulation of extracellular potassium. These effects depolarize the membrane of pyramidal cells in seizurogenic areas such as the CA3, which removes the Mg^{2+}-dependent NMDA receptor blockade, and along with increased AMPA/kainate receptor activation, leading to seizures which spread to areas, such as the CA1, susceptible to energy failure and cell death (Fig. 8).

Acknowledgments

This work was supported by grant funds from JDRF (1-2010-136).

References

Anon, 1994. Effect of intensive diabetes treatment on the development and progression of long-term complications in adolescents with insulin-dependent diabetes mellitus: Diabetes Control and Complications Trial. Diabetes Control and Complications Trial Research Group. J. Pediatr. 125, 177–188.

Anon, 1997. Hypoglycemia in the Diabetes Control and Complications Trial. The Diabetes Control and Complications Trial Research Group. Diabetes 46, 271–286.

Abdelmalik, P.A., et al., 2007. Hypoglycemic seizures during transient hypoglycemia exacerbate hippocampal dysfunction. Neurobiol. Dis. 26, 646–660.

Anderson, W.W., et al., 1986. Magnesium-free medium activates seizure-like events in the rat hippocampal slice. Brain Res. 398, 215–219.

Arieff, A.I., et al., 1974. Mechanisms of seizures and coma in hypoglycemia. Evidence for a direct effect of insulin on electrolyte transport in brain. J. Clin. Investig. 54, 654–663.

Astrup, J., Norberg, K., 1976. Potassium activity in cerebral cortex in rats during progressive severe hypoglycemia. Brain Res. 103, 418–423.

Auer, R.N., 2004. Hypoglycemic brain damage. Metab. Brain Dis. 19, 169–175.

Auer, R.N., et al., 1985a. The temporal evolution of hypoglycemic brain damage. I. Light- and electron-microscopic findings in the rat cerebral cortex. Acta Neuropathol. 67, 13–24.

Auer, R.N., et al., 1985b. The temporal evolution of hypoglycemic brain damage. II. Light- and electron-microscopic findings in the hippocampal gyrus and subiculum of the rat. Acta Neuropathol. 67, 25–36.

Auer, R.N., et al., 1984. Hypoglycemic brain injury in the rat. Correlation of density of brain damage with the EEG isoelectric time: a quantitative study. Diabetes 33, 1090–1098.

Avila-Fematt, F.M., Montana-Alvarez, M., 2010. Hypoglycemia in the elderly with diabetes mellitus. Rev. Investig. Clin. 62, 366–374.

Avoli, M., et al., 1996. Extracellular free potassium and calcium during synchronous activity induced by 4-aminopyridine in the juvenile rat hippocampus. J. Physiol. 493, 707–717.

Bakken, I.J., et al., 1998. [U-13C]glutamate metabolism in astrocytes during hypoglycemia and hypoxia. J. Neurosci. Res. 636–645 (United States).

Baloyannis, S.J., et al., 1987. Synaptic alterations in the acoustic cortex of the rat following insulin-induced hypoglycemia. Arch. Otorhinolaryngol. 244, 36–43.

Banting, F.G., et al., 1922. Pancreatic extracts in the treatment of diabetes mellitus. Can. Med. Assoc. J. 12, 141–146.

Basarsky, T.A., et al., 1999. Glutamate release through volume-activated channels during spreading depression. J. Neurosci. 19, 6439–6445.

Beenhakker, M.P., Huguenard, J.R., 2009. Neurons that fire together also conspire together: is normal sleep circuitry hijacked to generate epilepsy? Neuron 62, 612–632.

Behrens, C.J., et al., 2005. Induction of sharp wave–ripple complexes in vitro and reorganization of hippocampal networks. Nat. Neurosci. 8, 1560–1567.

Bree, A.J., et al., 2009. Diabetes increases brain damage caused by severe hypoglycemia. Am. J. Physiol. Endocrinol. Metab. 297, E194–E201.

Bures, J., et al., 1984. The meaning and significance of Leao's spreading depression. An. Acad. Bras. Cienc. 56, 385–400.

Burns, C.M., et al., 2008. Patterns of cerebral injury and neurodevelopmental outcomes after symptomatic neonatal hypoglycemia. Pediatrics 122, 65–74.

Butcher, S.P., et al., 1987. Cellular origins of endogenous amino acids released into the extracellular fluid of the rat striatum during severe insulin-induced hypoglycemia. J. Neurochem. 48, 722–728.

Butler, T.R., et al., 2010. Selective vulnerability of hippocampal cornu ammonis 1 pyramidal cells to excitotoxic insult is associated with the expression of polyamine-sensitive N-methyl-D-aspartate-type glutamate receptors. Neuroscience 165, 525–534.

Calabresi, P., et al., 1997. A possible mechanism for the aglycemia-induced depression of glutamatergic excitation in the striatum. J. Cereb. Blood Flow Metab. 17, 1121–1126.

Carey, M.E., et al., 1981. The effect of severe hypoglycemia upon cerebrospinal fluid formation, ventricular iodide clearance, and brain electrolytes in rabbits. J. Neurosurg. 54, 370–379.

Chiovini, B., et al., 2010. Enhanced dendritic action potential backpropagation in parvalbumin-positive basket cells during sharp wave activity. Neurochem. Res. 35, 2086–2095.

Crepel, V., et al., 1992. Developmental and regional differences in the vulnerability of rat hippocampal slices to lack of glucose. Neuroscience 47, 579–587.

Cryer, P.E., 2010. Hypoglycemia in type 1 diabetes mellitus. Endocrinol. Metab. Clin. N. Am. 39, 641–654.

Del Campo, M., et al., 2009. Seizure-like activity in the hypoglycemic rat: lack of correlation with the electroencephalogram of free-moving animals. Epilepsy Res. 83, 243–248.

Derchansky, M., et al., 2006. Bidirectional multisite seizure propagation in the intact isolated hippocampus: the multifocality of the seizure "focus". Neurobiol. Dis. 312–328 (United States).

El-Hayek, Y.H., et al., 2013. Hippocampal excitability is increased in aged mice. Exp. Neurol. 710-9 (Elsevier Inc, United States, 2013).

Ellender, T.J., et al., 2010. Priming of hippocampal population bursts by individual perisomatic-targeting interneurons. J. Neurosci. 30, 5979–5991.

Facci, L., Leon, A., Skaper, S.D., 1990. Hypoglycemic neurotoxicity in vitro: involvement of excitatory amino acid receptors and attenuation by monosialoganglioside GM1. Neuroscience 37 (3), 709–716 PubMed PMID: 1978930.

Fan, P., et al., 1988. Effect of low glucose concentration on synaptic transmission in the rat hippocampal slice. Brain Res. Bull. 21, 741–747.

Fanelli, C.G., et al., 2004. Insulin therapy and hypoglycaemia: the size of the problem. Diabetes Metab. Res. Rev. 20, S32–S42.

Fifková, E., Bures, J., 1964. Spreading depression in the mammalian striatum. Arch. Physiol. Biochem. 72, 171–179.

Footitt, D.R., Newberry, N.R., 1998. Cortical spreading depression induces an LTP-like effect in rat neocortex in vitro. Brain Res. 781, 339–342.

Gee, C.E., et al., 2010. Energy deprivation transiently enhances rhythmic inhibitory events in the CA3 hippocampal network in vitro. Neuroscience 168, 605–612.

Gibbs, F.A., Murray, E.L., 1954. Hypoglycemic convulsions three case reports. Electroencephalogr. Clin. Neurophysiol. 6, 674–678.

Haces, M.L., et al., 2010. Selective vulnerability of brain regions to oxidative stress in a non-coma model of insulin-induced hypoglycemia. Neuroscience 165, 28–38.

Hajos, N., et al., 2009. Maintaining network activity in submerged hippocampal slices: importance of oxygen supply. Eur. J. Neurosci. 29, 319–327.

Hajos, N., et al., 2013. Input–output features of anatomically identified CA3 neurons during hippocampal sharp wave/ripple oscillation in vitro. J. Neurosci. 33, 11677–11691.

Huberfeld, G., Menendez de la Prida, L., Pallud, J., Cohen, I., Le Van Quyen, M., Adam, C., Clemenceau, S., Baulac, M., Miles, R., 2011 May. Glutamatergic pre-ictal discharges emerge at the transition to seizure in human epilepsy. Nat Neurosci. 14, 627–634.

Ichord, R.N., et al., 2001. MK801 decreases glutamate release and oxidative metabolism during hypoglycemic coma in piglets. Brain Res. Dev. Brain Res. 128, 139–148.

Isaev, N.K., et al., 2007. Cellular mechanisms of brain hypoglycemia. Biochemistry-Russia 72, 471–478.

Izumi, Y., et al., 1994. Effects of lactate and pyruvate on glucose deprivation in rat hippocampal slices. Neuroreport 5, 617–620.

Jonas, P., et al., 1993. Quantal components of unitary EPSCs at the mossy fibre synapse on CA3 pyramidal cells of rat hippocampus. J. Physiol. 472, 615–663.

Kager, H., et al., 2002. Conditions for the triggering of spreading depression studied with computer simulations. J. Neurophysiol. 88, 2700–2712.

Karlocai, M.R., et al., 2014. Physiological sharp wave–ripples and interictal events in vitro: what's the difference? Brain 137, 463–485.

Kim, J.H., et al., 2007. Depletion of ATP and release of presynaptic inhibition in the CA1 region of hippocampal slices during hypoglycemic hypoxia. Neurosci. Lett. 411, 56–60.

Knopfel, T., et al., 1990. Cytosolic calcium during glucose deprivation in hippocampal pyramidal cells of rats. Neurosci. Lett. 117, 295–299.

Kofuji, P., Newman, E.A., 2004. Potassium buffering in the central nervous system. Neuroscience 1045–1056 (United States).

Lacherade, J.C., et al., 2009. An overview of hypoglycemia in the critically ill. J. Diabetes Sci. Technol. 3, 1242–1249.

Lapenta, L., et al., 2010. Focal epileptic seizure induced by transient hypoglycaemia in insulin-treated diabetes. Epileptic Disord. 12, 84–87.

Lauritzen, M., et al., 2011. Clinical relevance of cortical spreading depression in neurological disorders: migraine, malignant stroke, subarachnoid and intracranial hemorrhage, and traumatic brain injury. J. Cereb. Blood Flow Metab. 31, 17–35.

Lauritzen, M., et al., 1988. Quisqualate, kainate and NMDA can initiate spreading depression in the turtle cerebellum. Brain Res. 475, 317–327.

Leinekugel, X., et al., 1999. GABA is the principal fast-acting excitatory transmitter in the neonatal brain. Adv. Neurol. 79, 189–201.

Lewis, L.D., et al., 1974. Cerebral energy state in insulin-induced hypoglycemia, related to blood glucose and to EEG. J. Neurochem. 23, 673–679.

Loracher, C., Lux, H.D., 1974. Impaired hyperpolarising inhibition during insulin hypoglycaemia and fluoroacetate poisoning. Brain Res. 69, 164–169.

MacLeod, K.M., et al., 1993. Frequency and morbidity of severe hypoglycaemia in insulin-treated diabetic patients. Diabet. Med. 10, 238–245.

Maier, N., et al., 2003. Cellular and network mechanisms underlying spontaneous sharp wave–ripple complexes in mouse hippocampal slices. J. Physiol. 550, 873–887.

Marrannes, R., et al., 1988. Evidence for a role of the N-methyl-D-aspartate (NMDA) receptor in cortical spreading depression in the rat. Brain Res. 457, 226–240.

Mayer, M.L., et al., 1992. Pharmacologic properties of NMDA receptors. Ann. N. Y. Acad. Sci. 648, 194–204.

McBain, C.J., 1994. Hippocampal inhibitory neuron activity in the elevated potassium model of epilepsy. J. Neurophysiol. 72, 2853–2863.

Monaghan, D.T., et al., 1983. Anatomical distributions of four pharmacologically distinct 3H-L-glutamate binding sites. Nature 306, 176–179.

Montassir, H., et al., 2009. Associated factors in neonatal hypoglycemic brain injury. Brain Dev. 31, 649–656.

Nellgard, B., Wieloch, T., 1992. Cerebral protection by AMPA- and NMDA-receptor antagonists administered after severe insulin-induced hypoglycemia. Exp. Brain Res. 92, 259–266.

Ovalle, F., et al., 1998. Brief twice-weekly episodes of hypoglycemia reduce detection of clinical hypoglycemia in type 1 diabetes mellitus. Diabetes 47, 1472–1479.
Papagapiou, M.P., Auer, R.N., 1990. Regional neuroprotective effects of the NMDA receptor antagonist MK-801 (dizocilpine) in hypoglycemic brain damage. J. Cereb. Blood Flow Metab. 10, 270–276.
Rao, R., et al., 2010. Neurochemical changes in the developing rat hippocampus during prolonged hypoglycemia. J. Neurochem. 728–738 (England).
Sadgrove, M.P., et al., 2007. Effects of relative hypoglycemia on LTP and NADH imaging in rat hippocampal slices. Brain Res. 1165, 30–39.
Sakel, M., 1938. Insulin therapy in the future of psychiatry. Can. Med. Assoc. J. 39, 178–179.
Sandberg, M., et al., 1986. Extracellular overflow of neuroactive amino acids during severe insulin-induced hypoglycemia: in vivo dialysis of the rat hippocampus. J. Neurochem. 47, 178–184.
Saransaari, P., Oja, S.S., 1997. Enhanced GABA release in cell-damaging conditions in the adult and developing mouse hippocampus. Int. J. Dev. Neurosci. 163–174 (England).
Semyanov, A., Godukhin, O., 2001. Epileptiform activity and EPSP-spike potentiation induced in rat hippocampal CA1 slices by repeated high-K(+): involvement of ionotropic glutamate receptors and Ca(2+)/calmodulin-dependent protein kinase II. Neuropharmacology 40, 203–211.
Sheardown, M.J., 1993. The triggering of spreading depression in the chicken retina: a pharmacological study. Brain Res. 607, 189–194.
Sherin, A., et al., 2012. Cholinergic and GABAergic receptor functional deficit in the hippocampus of insulin-induced hypoglycemic and streptozotocin-induced diabetic rats. Neuroscience 69–76 (2011 IBRO. Published by Elsevier Ltd, United States).
Shin, B.S., et al., 2010. Prevention of hypoglycemia-induced neuronal death by hypothermia. J. Cereb. Blood Flow Metab. 30, 390–402.
Shoji, S., et al., 1992. Effect of glucose-depletion on excitatory synaptic transmission in the suprachiasmatic nucleus of the rat. Kurume Med. J. 39, 209–212.
Sieber, F.E., et al., 1993. Extracellular potassium activity and cerebral blood flow during moderate hypoglycemia in anesthetized dogs. Am. J. Physiol. 264, H1774–H1780.
Smith, J.M., et al., 2006. Physiological studies of cortical spreading depression. Biol. Rev. Camb. Philos. Soc. 81, 457–481.
Somjen, G.G., 2001. Mechanisms of spreading depression and hypoxic spreading depression-like depolarization. Physiol. Rev. 81, 1065–1096.
Somjen, G.G., et al., 1992. Mechanism of spreading depression: a review of recent findings and a hypothesis. Can. J. Physiol. Pharmacol. 70, S248–S254.
Spuler, A., et al., 1988. Glucose depletion hyperpolarizes guinea pig hippocampal neurons by an increase in potassium conductance. Exp. Neurol. 100, 248–252.
Stanika, R.I., et al., 2010. Differential NMDA receptor-dependent calcium loading and mitochondrial dysfunction in CA1 vs. CA3 hippocampal neurons. Neurobiol. Dis. 37, 403–411.
Tasker, R.C., et al., 1992. The regional vulnerability to hypoglycemia-induced neurotoxicity in organotypic hippocampal culture: protection by early tetrodotoxin or delayed MK-801. J. Neurosci. 12, 4298–4308.
Tekkok, S.B., et al., 2002. Moderate hypoglycemia aggravates effects of hypoxia in hippocampal slices from diabetic rats. Neuroscience 113, 11–21.
Tokizane, T., 1957. Sites of origin of hypoglycemic seizures in the rabbit. A.M.A. Arch. Neurol. Psychiatry 77, 259–266.
Tossman, U., et al., 1985. Gamma-aminobutyric acid and taurine release in the striatum of the rat during hypoglycemic coma, studied by microdialysis. Neurosci. Lett. 62, 231–235.
Velisek, L., et al., 2008. Metabolic environment in substantia nigra reticulata is critical for the expression and control of hypoglycemia-induced seizures. J. Neurosci. 28, 9349–9362.
Westbrook, G.L., Lothman, E.W., 1983. Cellular and synaptic basis of kainic acid-induced hippocampal epileptiform activity. Brain Res. 273, 97–109.
Wieloch, T., 1985. Hypoglycemia-induced neuronal damage prevented by an N-methyl-D-aspartate antagonist. Science 230, 681–683.
Wieloch, T., et al., 1984. Influence of severe hypoglycemia on brain extracellular calcium and potassium activities, energy, and phospholipid metabolism. J. Neurochem. 43, 160–168.
Wong, T., et al., 2005. Postnatal development of intrinsic GABAergic rhythms in mouse hippocampus. Neuroscience 134, 107–120.
Wu, C., et al., 2005a. An in vitro model of hippocampal sharp waves: regional initiation and. J. Neurophysiol. 94, 741–753.
Wu, C., et al., 2005b. An in vitro model of hippocampal sharp waves: regional initiation and intracellular correlates. J. Neurophysiol. 94, 741–753.
Wu, C., et al., 2005c. Size does matter: generation of intrinsic network rhythms in thick mouse hippocampal slices. J. Neurophysiol. 93, 2302–2317.
Wu, C., et al., 2002. A fundamental oscillatory state of isolated rodent hippocampus. J. Physiol. 540, 509–527.
Wu, C., et al., 2009. Adenosine as an endogenous regulating factor of hippocampal sharp waves. Hippocampus 19, 205–220.
Wu, C.P., et al., 2006. Spontaneous rhythmic field potentials of isolated mouse hippocampal–subicular–entorhinal cortices in vitro. J. Physiol. 576, 457–476.
Wuerthele, S.M., et al., 1978. A histological study of kainic acid-induced lesions in the rat brain. Brain Res. 149, 489–497.
Yaari, Y., et al., 1983. Spontaneous epileptiform activity of CA1 hippocampal neurons in low extracellular calcium solutions. Exp. Brain Res. 51, 153–156.
Zhang, Z.J., et al., 2012. Transition to seizure: ictal discharge is preceded by exhausted presynaptic GABA release in the hippocampal CA3 region. J. Neurosci. 32, 2499–2512.
Zhao, Y.T., et al., 1997. 2-Deoxy-D-glucose-induced changes in membrane potential, input resistance, and excitatory postsynaptic potentials of CA1 hippocampal neurons. Can. J. Physiol. Pharmacol. 75, 368–374.
Zhou, N., et al., 2013. Regenerative glutamate release by presynaptic NMDA receptors contributes to spreading depression. J. Cereb. Blood Flow Metab. 1582–1594.